

UvA-DARE (Digital Academic Repository)

Lanthanide-Based Metal Organic Frameworks: Synthetic Strategies and Catalytic Applications

Pagis, C.; Ferbinteanu, M.; Rothenberg, G.; Tanase, S.

DOI

[10.1021/acscatal.6b01935](https://doi.org/10.1021/acscatal.6b01935)

Publication date

2016

Document Version

Final published version

Published in

ACS Catalysis

License

Article 25fa Dutch Copyright Act

[Link to publication](#)

Citation for published version (APA):

Pagis, C., Ferbinteanu, M., Rothenberg, G., & Tanase, S. (2016). Lanthanide-Based Metal Organic Frameworks: Synthetic Strategies and Catalytic Applications. *ACS Catalysis*, 6(9), 6063-6072. <https://doi.org/10.1021/acscatal.6b01935>

General rights

It is not permitted to download or to forward/distribute the text or part of it without the consent of the author(s) and/or copyright holder(s), other than for strictly personal, individual use, unless the work is under an open content license (like Creative Commons).

Disclaimer/Complaints regulations

If you believe that digital publication of certain material infringes any of your rights or (privacy) interests, please let the Library know, stating your reasons. In case of a legitimate complaint, the Library will make the material inaccessible and/or remove it from the website. Please Ask the Library: <https://uba.uva.nl/en/contact>, or a letter to: Library of the University of Amsterdam, Secretariat, Singel 425, 1012 WP Amsterdam, The Netherlands. You will be contacted as soon as possible.

UvA-DARE is a service provided by the library of the University of Amsterdam (<https://dare.uva.nl>)

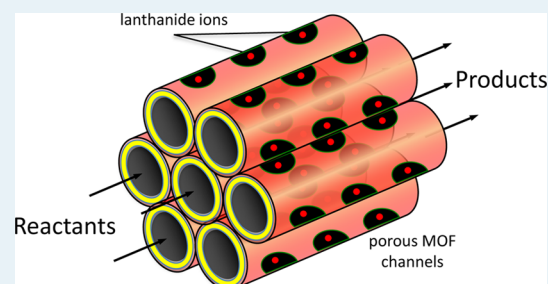
Lanthanide-Based Metal Organic Frameworks: Synthetic Strategies and Catalytic Applications

Céline Pagis,^{†,§} Marilena Ferbinteanu,[‡] Gadi Rothenberg,[†] and Stefania Tanase^{*,†}

[†]Van 't Hoff Institute for Molecular Sciences, University of Amsterdam, Science Park 904, 1098 XH Amsterdam, The Netherlands

[‡]Faculty of Chemistry, Inorganic Chemistry Department, University of Bucharest, Dumbrava Rosie 23, Bucharest 020462, Romania

ABSTRACT: This short critical review outlines the main synthetic strategies used in the designed synthesis of lanthanide-based metal organic frameworks (Ln-MOFs). It explains the impact of the choice of organic linker on the final network topology, and it highlights the applications of Ln-MOFs in the catalysis of organic reactions.



KEYWORDS: lanthanide, metal–organic frameworks, heterogeneous catalysis, Lewis acid

INTRODUCTION

Lanthanide coordination compounds are attractive Lewis acid catalysts in organic synthesis.¹ Their labile lanthanide-to-oxygen bonds favor ready dissociation of substrates, allowing catalysis with high turnovers. Specifically, lanthanide triflates are considered a promising class of green catalysts because they are very stable in water and easily recovered.² These catalysts are highly effective in Fridel–Crafts,³ Diels–Alder,⁴ aldol, allylation, and Michael addition⁵ reactions.

Using lanthanide coordination compounds as catalysts in organic chemistry is an expanding research field, mainly due to their efficacy as Lewis acid catalysts.⁶ Recent research has demonstrated their value as homogeneous catalysts.⁷ This is an important achievement because water-stable Lewis acid catalysts can reduce the environmental impact of the chemical industry significantly.^{2,5} The lanthanide series shows a regular variation of Lewis acidity, which can be tuned by choosing the proper ligand. Moreover, the high and variable coordination numbers of lanthanide ions allow easy rearrangements for substrate activation.⁶ Lanthanide compounds are also readily recovered and can be reused, lowering their environmental impact.⁸

Many kinds of solid Lewis acid catalysts have been developed.⁹ However, most of these require strictly anhydrous conditions. Performing catalytic reactions using solid Lewis acids in water is attractive because they are insoluble and can be much easier removed from the products.^{9a} While many zeolites and metal oxides have Lewis acid sites, these are generally inactive sites for reactions in water due to the formation of Lewis acid–base adducts by the coordination of water to the acid sites. In this respect, lanthanide-based metal organic frameworks (MOFs) are appealing candidates. MOFs are three-dimensional porous structures made of metal ions or clusters of ions linked by organic molecules. They share some of the

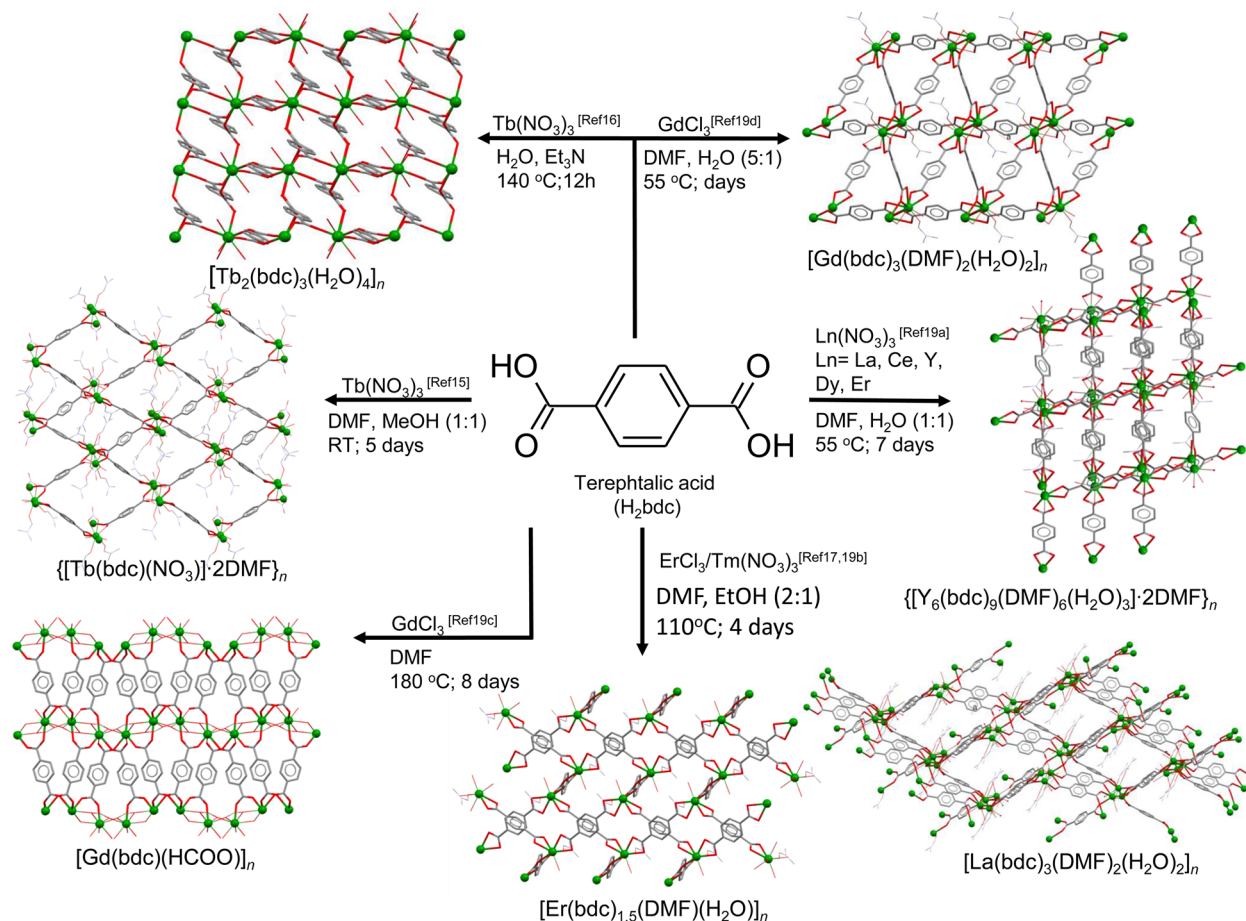
catalytically relevant features of zeolites (large internal surface areas and uniform pore and cavity sizes), but they also have important differences. MOFs contain organic components and therefore can be synthesized in much greater chemical variety than zeolites.¹⁰ Some of the lanthanide-based MOFs are water-stable and even more stable than their transition-metal-based analogues.¹¹

Compared with the well-established syntheses of MOFs based on transition-metal ions, less is reported on synthetic strategies for making lanthanide-based MOFs (Ln-MOFs).¹² Their physics and luminescence properties are covered in several excellent recent reviews.¹³ Transition-metal ions have well-understood geometrical characteristics, facilitating network design. Conversely, lanthanide ions have large coordination numbers and flexible coordination geometries. Making porous solids is challenging because the enthalpy will always favor a dense material. Nevertheless, binding solvent molecules to lanthanide ions in MOFs is highly favorable thanks to their large coordination numbers. These facilitate the removal of the solvent molecules without framework collapse. Thus, it enables the formation of porous solids with Lewis acid centers and coordinatively unsaturated sites, which can then be used for catalysis.

To realize this catalytic potential of Ln-MOFs, strategies must be developed for building large-pore and high-surface-area structures. Here, we present an overview of the main synthetic strategies for obtaining highly stable and porous Ln-MOFs as well as their applications in catalysis.

Received: July 11, 2016

Published: July 25, 2016

Scheme 1. Examples of MOFs Built from Lanthanide Ions and Benzene-1,4-dicarboxylic Acid ($H_2\text{bdc}$)

■ STRATEGIES FOR DESIGNING LN-MOFS

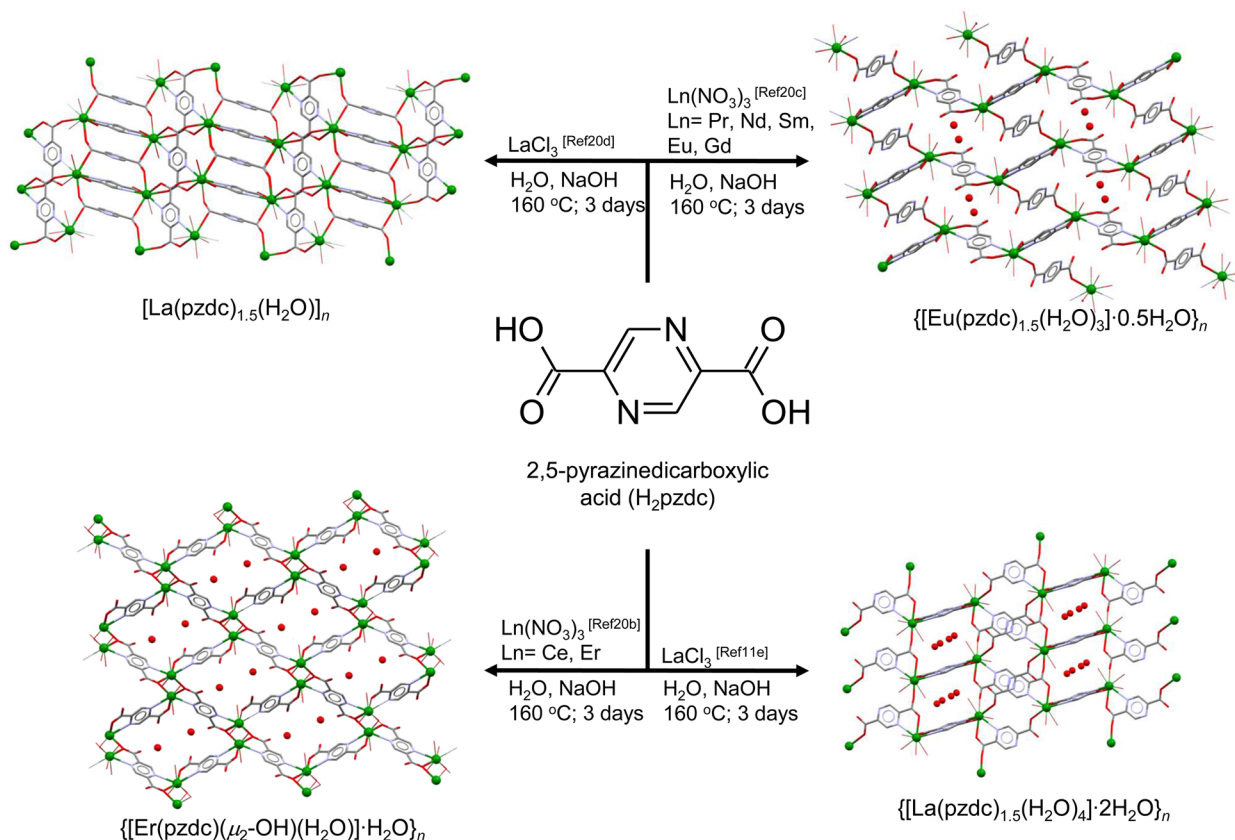
Direct Synthesis from Rigid Linkers. The first choice when designing a porous structure are the directional and rigid ligands. Among these, aromatic ligands with carboxylate functional groups are preferred, as they allow the formation of robust frameworks. Moreover, carboxylates satisfy the oxophilic nature of the lanthanide ions, and their ability to bind in various modes suit well the lack of preferred coordination geometry of the lanthanide ions. In a typical Ln-MOF synthesis, the lanthanide salt and the carboxylate ligand are combined in the desired stoichiometry. The reaction is usually run above 120 °C when the acid is poorly soluble. In some cases, a base is needed to deprotonate the ligand. The process is typically run in water, dipolar aprotic solvents (DMF, DEF, or DMSO) or mixtures thereof. A variety of organic ligands have been used in combination with lanthanide ions.^{12b,d-f,i,14} However, few of these gave thermally stable porous networks that did not collapse after removing the guest solvent molecules. These successful examples are discussed below.

In 1999, Yaghi et al.¹⁵ reported the synthesis of the first Ln-MOF, $[\text{Tb}(\text{bdc})(\text{NO}_3)] \cdot 2\text{DMF}$ ($H_2\text{bdc}$ = benzene-1,4-dicarboxylic acid). The framework topology is best described as a simple (3,4)-connected network (see Scheme 1). The 4-connected vertices are the terbium atoms which are connected through the oxygen of the carboxylate groups of the bdc ligand (the 3-connected vertices). These are in turn joined in pairs by the $-\text{C}_6\text{H}_4-$ links. The desolvated form is a microporous framework which retains the original topology and it is stable

up to 450 °C.¹⁵ Its immersion in water gives an irreversible and quantitative conversion to another material, $[\text{Tb}_2(\text{bdc})_3] \cdot 4\text{H}_2\text{O}$, which has extended 1D channels.¹⁶ Upon dehydration, this material retains its porosity, with accessible metal sites within the pores.¹⁶

Combining the bdc linker with smaller lanthanide ions, for example, Er(III), gives a different structural topology.¹⁷ The compound $[\text{Er}(\text{bdc})_{1.5}(\text{DMF})(\text{H}_2\text{O})]_n$ has a 3D nonporous framework formed by the interpenetration of (4,6)-connected topology (see Scheme 1).¹⁷ This interpenetration can be avoided, however, by introducing two additional hydroxyl groups in the bdc ligand. Thus, $[\text{Er}_2(\text{dhbdc})_3(\text{DMF})_3] \cdot 2\text{DMF}$ has a porous (4,6)-connected network in which $\text{Ln}_2(\text{COO})_6$ dinuclear units are linked by $-\text{C}_6\text{H}_2(\text{OH})_2-$ spacers.¹⁸ The resulting 3D framework has 1D open channels that accommodate the DMF guest molecules. Another strategy for preventing the network interpenetration involves replacing the coordinated solvents by chelating ligands, for example, 1,10-phenanthroline (phen).¹⁷ Using bdc as the linker, a variety of network topologies were obtained for the Ln-MOFs, depending on the reaction conditions.¹⁹

A variety of functional architectures can also be built by introducing more functionality in the organic linker. Thus, the fully deprotonated pyrazine-2,5-dicarboxylic linker (pzdc) affords six donor atoms, which give rise to various architectures upon coordination to lanthanide ions (see Scheme 2 for details).^{11e,20} Likewise, the nature of the lanthanide salt used as well as the reaction conditions play a key role in defining the final architecture. We recently showed that the MOF

Scheme 2. Examples of MOFs Built from Lanthanide Ions and Pyrazine-2,5-dicarboxylic Acid (H_2pzdc)

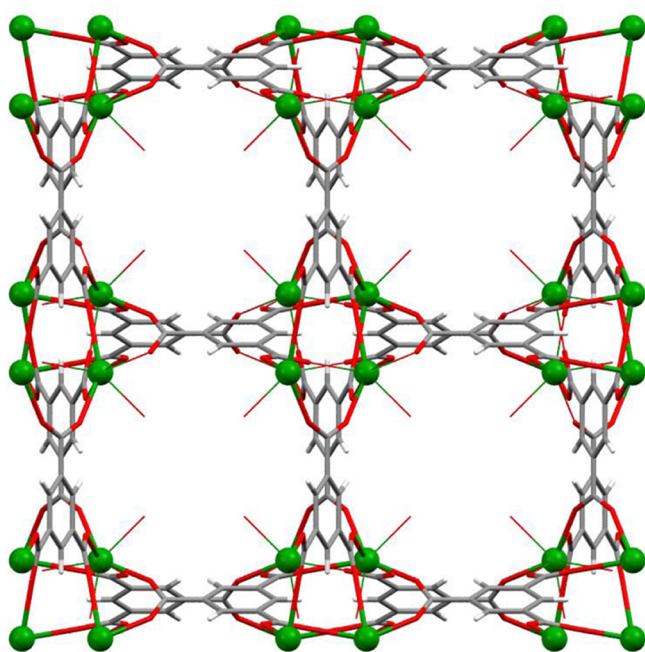
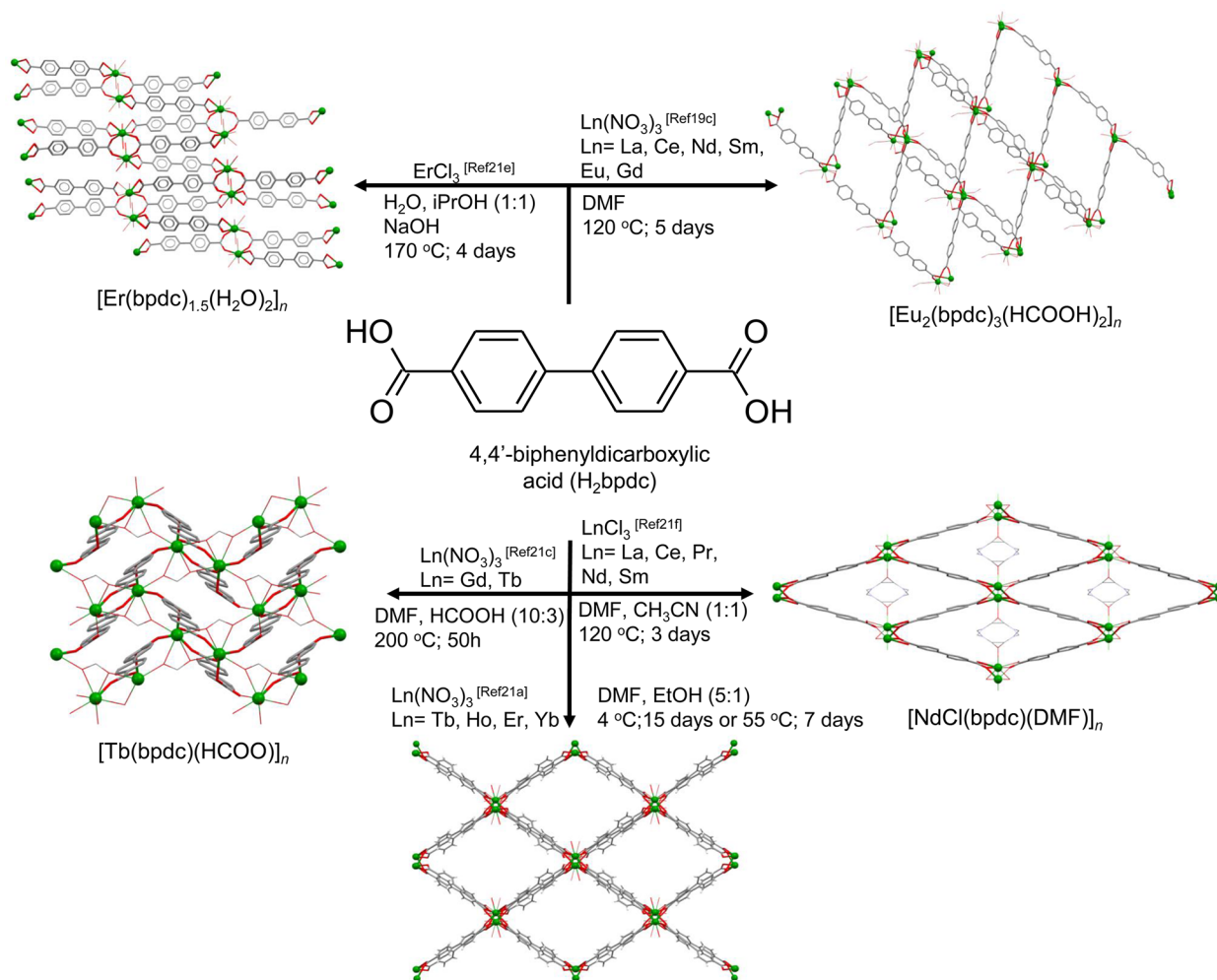
$[La(pzdc)_{1.5}(H_2O)] \cdot 2H_2O$ easily accommodates water and withstands several hydration/dehydration cycles.^{11e}

The size of the pores and the voids in the framework can be controlled by choosing the appropriate length of the linker. Several studies aimed at making Ln-MOFs using 4,4'-biphenyldicarboxylic acid (H_2bpdc) as linker. Most of these compounds have 3D sandwich structures (see Scheme 3).²¹ In one case, a MOF structure with relatively high pores, ca. $17 \times 25 \text{ \AA}^2$, was obtained by careful control of the reaction conditions.^{21a} The large torsion angle of the phenyl rings of the $bpdc$ linker combined with $C-H \cdots \pi$ interactions between adjacent linkers give rise to an impenetrable wall of biphenyl groups.^{21a} Using longer linkers may also lead to the interpenetration of the framework and/or partial collapse of the framework upon removal of the guest molecules. Indeed, reacting $Tb(NO_3)_3$ and azobenzene-4,4'-dicarboxylic acid (H_2adb) leads to a doubly interpenetrating structure, where each framework has an idealized cubic 6-connected net.²² Despite the presence of two interpenetrating networks, 20 DMSO guest molecules occupy the pores (71% of the crystal volume). However, the desolvated material is unstable due to the linker's flexibility.

In some cases, increasing the number of phenyl rings in the linker also improves the thermal stability of both the linker and the corresponding Ln-MOF. This is seen in several Ln-MOFs built from tritopic ligands. Note, however, that this is not a general trend in MOFs chemistry because there are many competitive factors which govern MOFs both thermal and chemical stability. Ln-MOFs with a (6,6)-connected topology and unidimensional helical strands were prepared by reacting lanthanide nitrates with 1,3,5-benzenetricarboxylic acid (H_3btc ,

see Figure 1).²³ The helical strands are attributed to the steric orientation of the btc ligand carboxylate groups. These materials have surface areas of about $750 \text{ cm}^2/\text{g}$ and high voids of about 45%.²³ They have available metal sites and are stable up to $450 \text{ }^\circ\text{C}$. This makes them attractive candidates for catalytic applications. Using the same linker but varying the lanthanide ions and the reaction conditions gives diverse Ln-MOFs.²⁴ Notably, the crystal structure of $[Tb(btc)(H_2O)_{1.5}(DMF)]$ reveals rods constructed from seven-coordinated $Tb(III)$ ions.^{24a} These rods pack in tetragons giving square channels ($6.6 \times 6.6 \text{ \AA}^2$) accommodating DMF molecules.^{24a} Powder neutron diffraction studies show that an optimal pore size ($\sim 6 \text{ \AA}$) strengthens the interaction between dihydrogen molecules with pore walls, thus enhancing hydrogen adsorption.²⁵

Using an expanded version of the btc ligand, Walton et al.²⁶ obtained a stable and porous (4,6)-connected network, $[La(btb)(H_2O)] \cdot 3DMF$ (where $btb = 1,3,5\text{-tris}(4\text{-carboxyphenyl})benzene$). This material retains its framework after removal of the guest molecules. It is stable up to $560 \text{ }^\circ\text{C}$, making it the most stable porous Ln-MOF to date. Remarkably, it has a high surface area ($1014 \text{ m}^2/\text{g}$) and shows *breathing effects* upon N_2 and CO_2 adsorption.²⁶ The same ligand forms a (3,5)-connected network in combination with $Tb(III)$.²⁷ Edge-sharing TbO_9 polyhedra define rods that are connected by tritopic bdb ligands, giving unidimensional hexagonal channels.²⁷ Several microporous Ln-MOFs with btb -derived linkers were reported.²⁸ All of these are highly robust structures, with good thermal and chemical stabilities as well as remarkable selectivity in gas separation.^{28b-e}

Scheme 3. Examples of MOFs Built from Lanthanide Ions and 4,4'-Biphenyldicarboxylic Acid (H_2bpdC)Figure 1. Three-dimensional structure of $[Ln(btc)(H_2O)] \cdot 1.1DMF$.

The reaction of lanthanide nitrates with the more functionalized 4,4',4''-s-triazine-2,4,6-triyl-tribenzoate (tatb) ligand gives interpenetrated (8,3)-connected networks (see Figure 2).²⁹ Although they are stable up to 550 °C, the interpenetration restricts the pore size. Using the same ligand, $Tb(NO_3)_3$ and different reaction conditions, Kim et al.³⁰ obtained a mesoporous MOF containing cages of 3.9 and 4.7 nm in diameter. Here, the lanthanide ions and linkers are uniquely assembled, producing a zeotype network stable up to 120 °C and with a surface area of 1419 m²/g.³⁰

Combining carboxylate-substituted polychlorotriphenylmethyl (PTMTC) radicals with lanthanide ions, Veciana et al.³¹ synthesized a series of porous materials. These remarkable $\{[Ln((PTMTC)(EtOH)_2(H_2O)] \cdot xH_2O \cdot yEtOH\}$ compounds (where Ln = Eu, Gd, Tb) have a rare neutral 3D framework built from 6-connected Ln(III) paddle-wheel units and 3-connected radical nodes. Figure 3 shows the interconnection of these building units, and the corresponding 1D helical channels occupied by solvent molecules. The framework remains unchanged when the guest molecules are removed.^{31c}

MOFs containing lanthanide ions and tetracarboxylate ligands are rare.³² One example is the (4,8)-connected networks containing the methylenediisophthalate (MDIP) linker.^{32a} Here, $[Ln_2(COO)_8]^{2-}$ units are connected to the neighboring moieties through eight MDIP ligands, forming a 3D open framework with elliptical channels.

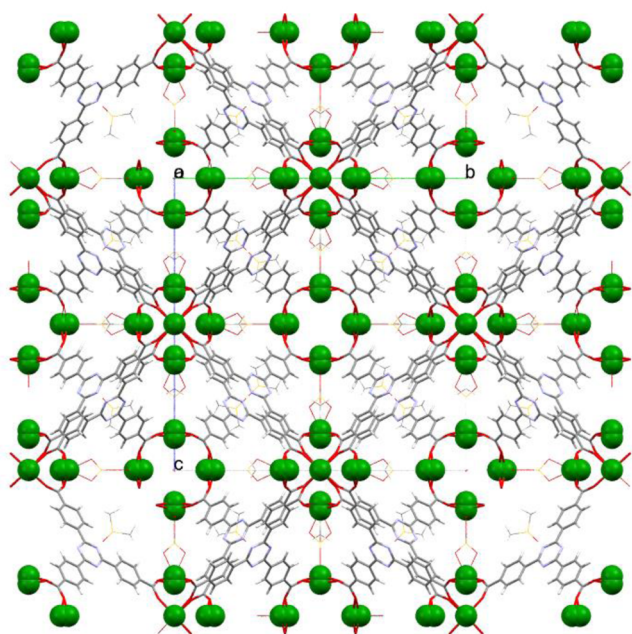


Figure 2. Interpenetrated networks of the lanthanide ions bound to the tatb ligand.

Isorecticular Synthesis. Yaghi et al.^{24a} showed that the permanent porosity of the MOFs is imparted by the structural properties of the metal–carboxylate clusters, where each metal is locked into position by carboxylates, giving rigid entities with simple geometries. These are the so-called *secondary building units* (SBUs). They are considered as the *joints* and the organic linkers as the *struts* of the underlying net when the MOFs structure is interpreted and/or predicted.^{24a} This approach allows designing MOFs by encoding the structural information in the building block itself. Interestingly, infinite rod-shaped SBUs containing Tb(III) ions do not interpenetrate due to the intrinsic packing arrangement in the crystal structure.^{24a,33} In $[\text{Tb}(\text{pdc})_{1.5}(\text{H}_2\text{O})_2(\text{DMF})]\cdot\text{DMF}$ (where Hpdc = 2,7-tetrahydropyrenedicarboxylic acid), the rods are composed of chains of eight-coordinated Tb(III) ions that form square anti-

prisms.^{24a} The rods are linked together by pdc connectors to give a primitive cubic (pcu) topology having $19.3 \times 5.8 \text{ \AA}^2$ channels.^{24a}

The ability of rod-shaped Ln–carboxylate chain SBUs to generate high-dimensional framework was shown in recent studies.^{14,34} Combining lanthanide ions and tritopic linkers gives a series of isorecticular Ln–MOFs with unidimensional pseudo-hexagonal channels.¹⁴ In these structures, the lanthanide ions are coordinated by six carboxylate groups belonging to six tritopic linkers.¹⁴ Each linker binds to three Ln–carboxylate chains, forming the unidimensional channel topology.¹⁴ Channel pore sizes vary from 8.4–23.9 Å. The Ln–carboxylate chains are highly rigid and therefore the expansion of the tritopic linkers allows control of the channel size.

Eddaoudi et al.^{34,35} showed that in situ-prepared hexanuclear or nonanuclear lanthanide clusters are excellent candidates for reticular synthesis. Reacting lanthanide ions and 2-fluorobenzoic acid (Hfba) gives highly stable hexanuclear clusters of the type $[\text{Ln}(\mu_3\text{-OH})_8(\text{O}_2\text{C-})_{12}]$.^{34c,35} When combined with ditopic rigid linkers, these SBUs form a series of 12-connected MOFs which have a face-centered cubic (fcc) topology (see Scheme 4 for details).³⁵ The carboxylate carbon atoms of the hexanuclear SBUs act as extension points and correspond to the vertices of the fcc topology.³⁵ Combining the same SBUs with various square-shaped tetracarboxylate ligands yields a series of isorecticular MOFs with ftw topology.^{34b} This topology can be viewed as a primitive cubic packing of the 12-connected SBUs, which are positioned in the center of the cell.^{34b} Each SBU is connected through 12 bis-monodentate carboxylate groups from 12 separate tetracarboxylate ligands.^{34b} The result is a central cubic cage, the diameter of which is delimited by six ligands (see Scheme 4 for details).^{34b} Reacting lanthanide ions and Hfba in the presence of a tritopic ligand gives a MOF built from nonanuclear SBUs of type $[\text{Ln}_9(\mu_3\text{-OH})_8(\mu_2\text{-OH})(\text{O}_2\text{C-})_{18}]$ (Scheme 4).^{34a}

Building-Block Approach. In 1990, Robson et al.³⁶ introduced the building-block approach for constructing polynuclear compounds. Since then, many research groups contributed to this field in terms of establishing design principles. Compared with the methods described above, the

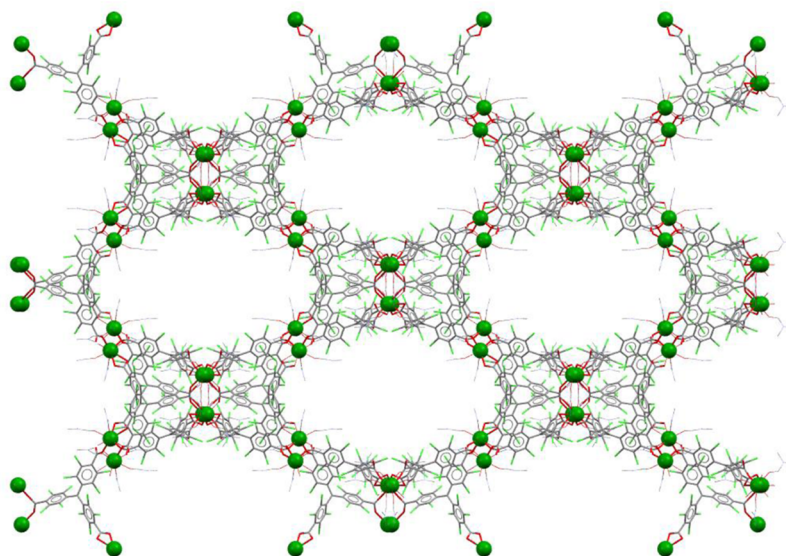
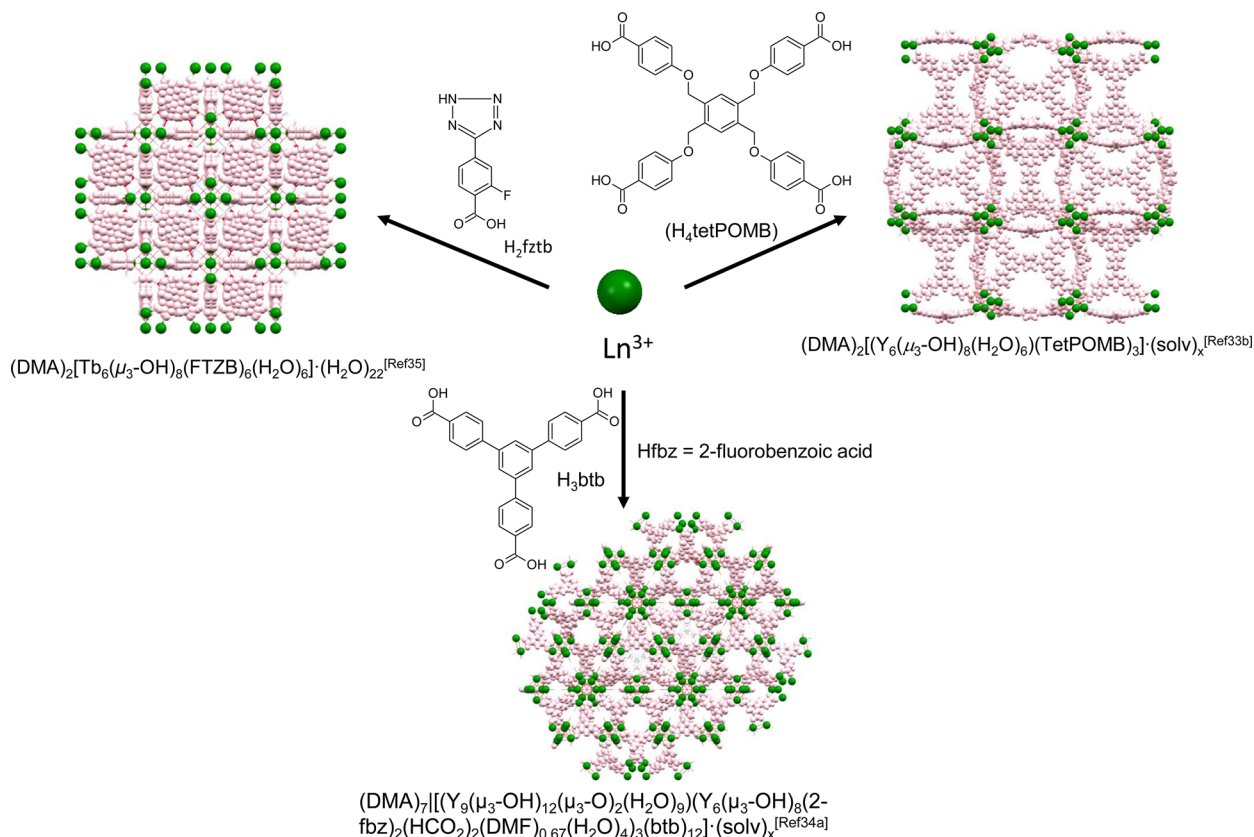


Figure 3. View of the 3D structure of $\{[\text{Eu}((\text{PTMTC})(\text{EtOH})_2(\text{H}_2\text{O}))\cdot x\text{H}_2\text{O}\cdot y\text{EtOH}]\}$.

Scheme 4. Isoreticular Synthesis of Ln-MOFs Using In Situ-Prepared Hexanuclear or Nonanuclear Lanthanide Clusters



construction of extended networks using the building-block strategy is usually done at or near room temperature. This means that the structural integrity of the building-block unit is maintained through the reaction. Although this approach is used successfully in the synthesis of MOFs containing transition-metal ions, its application to Ln-MOFs is less common. This is due to the variable coordination numbers and geometries of lanthanide ions.

Shimizu et al.³⁷ synthesized an isostructural series of Ln-MOFs using a stepwise assembly. Thus, lanthanide ions were initially reacted with the dianionic ligand 4,4'-disulfo-2,2'-bipyridine-*N,N'*-dioxide (L) to form building blocks of type $[\text{LnL}_3(\text{H}_2\text{O})_2]^{3-}$. Subsequently, the sulfonate groups were used as second binding sites to coordinate to Ba(II) ions. Cross-linking the $[\text{LnL}_3(\text{H}_2\text{O})_2]^{3-}$ units with barium ions resulted in the formation of microporous solids.³⁷ The crystal structure has open channels that readily adsorb/desorb water. This process is accompanied by a sponge-like shrinkage and expansion of the framework.³⁷ The average pore size is 6.4 Å, and the microporous structure was confirmed by CO₂ adsorption measurements (surface area 718 m²/g).³⁷

Recently, we developed a method for making Ln-MOFs using in situ-prepared lanthanide building blocks. Combining $[\text{Ln}(\text{mpca})_2(\text{solvent})_x]^+$ species (Hmpca = 5-methyl-2-pyrazinecarboxylic acid; solvent = H₂O, CH₃OH) with $[\text{M}(\text{CN})_8]^{4-}$ (M = Mo, W) building blocks gives robust porous networks with open channels (see Figure 4).³⁸ The crystal structure shows that the $[\text{M}(\text{CN})_8]^{4-}$ building block is connected to three $[\text{Ln}(\text{mpca})_2(\text{CH}_3\text{OH})]^+$ units, forming 2D networks that are connected through a second lanthanide ion.³⁸ The result is robust three-dimensional networks with one-dimensional channels (see Figure 4). These MOFs retain their crystallinity

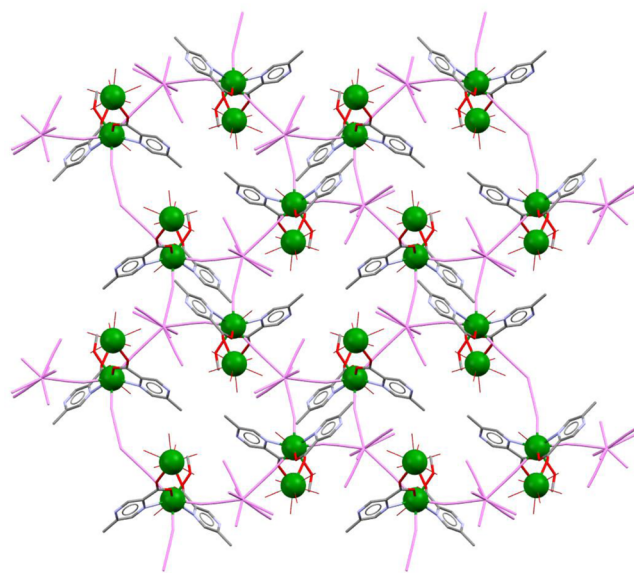
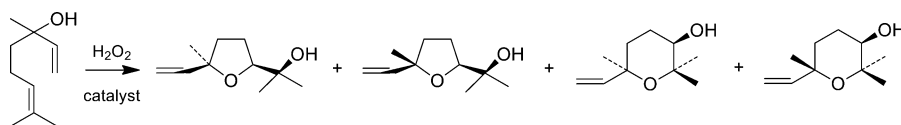


Figure 4. Three-dimensional structure of $[\text{Eu}(\text{mpca})_2(\text{CH}_3\text{OH})_2]\text{Eu}(\text{H}_2\text{O})_6\text{W}(\text{CN})_8 \cdot n\text{H}_2\text{O}$.

although structural rearrangements take place upon dehydration.^{38a} The CO₂ adsorption studies indicated a microporous structure with surfaces area of 160–200 m²/g. The highly hydrophilic nature of the one-dimensional channels makes these materials attractive candidates for proton transport applications.³⁹

Scheme 5. Catalytic Oxidation of Linalool to Hydroxyl Ethers



ORGANIC REACTIONS CATALYZED BY LANTHANIDE-BASED MOFs.

The main requirements of a MOF catalyst are keeping its framework structure during the catalysis and having open channels to allow efficient transport of reactants/products. Tuning pore sizes enables preferential uptake of the reactants, leading to selective catalytic activity. MOFs with large open channels are preferred, but such frameworks are often distorted when the guest molecules are removed. Nevertheless, the examples discussed above demonstrate that the design of Ln-MOFs with high surface area and large pores is possible, using both rigid and flexible organic linkers. However, none of these MOFs have been tested in organic reactions.

Although several Ln-MOFs catalysts are reported, only a few have proven porosity and/or are made by specific design with the purpose to catalyze a targeted organic reaction. In fact, there are two main synthetic strategies employed for making Ln-MOFs. One combines the Lewis acidity of lanthanide ions with a functional basic site on the organic linker.⁴⁰ The other focuses on increasing the overall acidity of the Ln-MOFs using the cooperative effects of the lanthanide Lewis acidity and an acidic group of the organic linker.⁴¹ We will discuss here only the most relevant and efficient catalytic reactions.

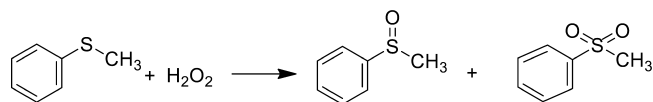
Oxidation Reactions. Olefin epoxidation is an important reaction because epoxides are key intermediates in many industrial processes. While the olefin epoxidation catalyzed by homogeneous lanthanide is well-studied,⁴² the same reaction catalyzed by heterogeneous catalysts has received less attention. Lanthanide carboxylate frameworks, [Ln(HCOO)₃] (Ln = Pr, Nd), were found to be active catalysts in the epoxidation of various cyclic and linear olefins with ^tBuOOH as oxidant.⁴³ These MOFs have equilateral triangular pores of 5.3 Å × 5.3 Å × 5.3 Å size. The oxidation of cyclopentene and 1-hexene showed almost complete conversion with the corresponding epoxide being the sole product.⁴³ For the long chain linear olefins, the conversion is limited to 38–42%.⁴³ Generally, the selectivity and conversion decrease as the bulkiness and chain length of the substrate increases. The bulky substrates cannot approach the active site easily, so it is likely that the catalytic reaction occurs within the pores. Other oxidants such as hydrogen peroxide and sodium hypochlorite were less efficient.⁴³

Several Ln-MOFs containing arenedisulfonate ligands were tested as catalysts in the epoxidation of linalool,^{41f,h,44} yielding a mixture of cyclic hydroxyl ether isomers (see Scheme 5). In all cases, a ratio of 2:3 is found between the furanoid and piranoid form of the final products. A full conversion of linalool was observed with [La(OH)(1,5-NDS)(H₂O)] where 1,5-NDS is 1,5-naphthalenedisulfonate.^{41f,h} The epoxidation of the 2,3-double bond occurs first, followed by the intramolecular opening of the epoxide ring by the hydroxyl group at positions 6 or 7. It is proposed that the first step is a lanthanide-catalyzed reaction and the second is catalyzed by the acidic sites of the organic linker (e.g., sulfonate groups).⁴⁴ This series of MOFs has a dense 3D structure, and therefore, their catalytic activity is driven by the bulk acidity, resulting from combined effect of

lanthanide Lewis acidity and the relatively strong acid character of the sulfonic groups of the organic linker. A correlation between the catalytic activity and the coordination number of the lanthanide ion was observed. The most active MOFs are those containing eight-coordinated Ln(III) ions.^{41f} This allows the lanthanide ion to reach higher coordination numbers during the catalytic process, thus increasing the catalytic efficiency. Notably, several Ln-MOFs containing ligands with sulfonic groups^{41a,c,f,h} were tested in a variety of organic reactions, but none of these have a porous structure.

The redox abilities of a few Ln-MOFs were tested in the oxidation of sulfides (see Scheme 6).^{41e,g,h,45} Oxidizing sulfides

Scheme 6. Oxidation of Methyl-Phenyl Sulphide Catalyzed by Ln-MOFs (See Also Reaction Data in Table 1)



to sulfoxides is of interest because sulfoxides are important chiral building blocks.⁴⁶ Sulfides were selectively mono-oxygenated to the corresponding sulfoxides, using dihydrogen peroxide as oxidant.^{41e,45a} Conversions of 50–100% were reached in the presence of a low amount of catalyst (Table 1).^{41e,g,h,45a} These reports suggest that the active catalyst is a lanthanide-peroxo species formed in situ.^{42,43,43} However, there are no in-depth studies supporting this hypothesis.^{41e,g,h}

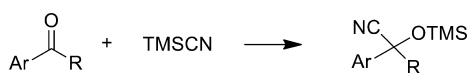
Table 1. Methyl-Phenyl Sulphide Oxidation with H₂O₂ Using Ln-MOFs

Ln-MOF	conversion (%)	time (min)	selectivity (%)	TOF (h ⁻¹)	ref
[Yb(C ₄ H ₄ O ₄) _{1.5}]	50	360	92	457	45a
[Yb ₂ (C ₁₇ H ₈ F ₆ O ₄) ₃]	92	180	30	60	41e
Yb-RPF5	100	30	90	706	41h
[La ₂ (C ₁₇ H ₈ F ₆ O ₄) ₃]	80	300	75	18	41e
La-RPF9	87	450	92	108	41g
Nd-RPF9	30	250	90	83	41g

Cyanosilylation Reactions. An important carbon–carbon reaction is the addition of cyanide to a carbonyl compound to form a cyanohydrin. This is because cyanohydrins are important synthetic intermediates for several organic compounds (e.g., α -hydroxyacids, α -hydroxyaldehydes, β -amino-alcohols).⁴⁷ The Lewis acid-catalyzed reaction of carbonyl compounds with cyanide affords the highly versatile cyanohydrin trimethylsilyl ethers (Scheme 7). These compounds can be readily converted into α -hydroxycarboxylic acids or β -amino alcohols.

A number of Ln-MOFs were tested in cyanosilylation reactions to explore their Lewis acid properties. Reacting benzaldehyde with cyanotrimethylsilane in the presence of [Sm(L-H₂)(L-H₃)(H₂O)₄·xH₂O] (L-H₄ = 2,2'-diethoxy-1,1'-binaphthalene-6,6'-bisphosphonic acid) gave mandelonitrile in

Scheme 7. Catalytic Cyanosilylation of Aldehydes or Ketones in the Presence of Ln-MOFs



69% yield.^{41d} Similar reactions performed with 1-naphthaldehyde and propionaldehyde gave lower yields (racemic mixtures were obtained in all cases).^{41d} The MOF catalyst, containing both Lewis and Brønsted acid sites, has a lamellar structure. The lamellae stack via interdigitation of binaphthyl rings from adjacent layers, giving large asymmetric channels with a diameter of ca. 12 Å. On the basis of the differences in the reaction yield, it was proposed that the catalytic activity depends on the size of the aldehydes and that the lamellar structure can swell, facilitating the substrate transport.^{41d}

The Tb(III) MOF built from tricarboxytriphenylamine (H₃tca) has both a high concentration of Tb(III) Lewis acid sites as well as Lewis basic triphenylamine sites.^{40c} The 1D channels of this MOF have a cross-section of 7.5 Å × 8.5 Å, large enough to host various substrates. Using Tb-tca as catalyst, the cyanosilylation of various aldehydes with cyanotrimethylsilane gives yield up to 98% within 16 h.^{40c} The highest conversion was obtained for 2-nitrobenzaldehyde, and the lowest for 1-naphthaldehyde, indicating a size-dependent activity. In fact, photophysical measurements showed that the Tb(III) ions play a key role in the adsorption and activation of aldehyde. The interaction of the 2-nitrobenzaldehyde with the catalyst frameworks results in the emission quenching of Tb(III) ion, while in the presence of bulkier substrates little or no quenching occurs. This shows the size selectivity effect in this cyanosilylation reaction.^{40c} Notably, the combined acid–base character of the Tb-tca MOF results in higher cyanosilylation reaction yield compared with the combined acid–acid character of bisphosphonates MOFs, which give only up to ca. 70% yield.^{41d}

The confined effect of the Tb-tca porous structure was also demonstrated in Knoevenagel reactions.^{40c} The reaction of salicylaldehyde with malonitrile has the highest conversion up to 99% while the conversion of 2-hydroxy-1-naphthaldehyde is reduced to about 20%. ¹H NMR studies have indeed confirmed that up to 3 equiv of salicylaldehyde are adsorbed inside the channels, compared with at most 1 equiv for bulkier aldehydes.

A similar size-dependent selectivity relationship was observed for the catalyst [Tb₆(H₃L)₄(NO₃)₉·3H⁺]⁶⁺ (H₃L = N',N',N''-tris(pyridin-2-ylmethylene)benzene-1,3,5-tricarbohydrazide, having a porous structure with 1D channels (ca. 11.5 Å diameter) and an acid–base character.^{40d} The cyanosilylation of nitrobenzaldehyde isomers gave up to 95% yield within 1.5 h, comparable with the activity of the Tb-tca MOF. The conversion of benzaldehyde was only 13%. As in the previous case, fluorescent titration studies showed that only suitably sized molecules can enter the pores.^{40d} These molecules interacted with the Tb(III) ions, giving a emission response that was used to determine the size-selectivity performance.^{40d}

Among the Ln-MOFs, [Nd(btc)(H₂O)]·0.5H₂O·DMF (pore size ca. 7.0 Å × 7.0 Å), is the most active catalyst in the cyanosilylation of benzaldehyde.^{11d} A conversion of 88% is reached after 1 h, and the catalyst is reusable at least five times.^{11d} However, when comparing with the two examples discussed above, it is very likely that the substrate activation occurs on the catalyst surface and not in its small pores. In fact, the catalytic activity decreases with the ionic radius of the

lanthanide ions along the series [Ln(btc)(H₂O)]·0.5H₂O·DMF.^{11d} This trend is opposite to that observed for the homogeneous triflate catalysts.⁴⁸ The difference was ascribed to the steric hindrances of the substrate when approaching the coordinatively unsaturated lanthanide ion of the MOF.^{11d}

The cyanosilylation of aldehydes under solvent-free conditions was studied in the presence of [Ln(3,5-dsb)(phen)] (Ln = La, Pr, Nd; 3,5-dsb = 3,5-disulfobenzoate; phen = 1,10-phenanthroline) as catalysts.^{41c} The reaction is ruled by the Lewis acid character of the catalyst bulk because the Nd(III) compound is more reactive than the Pr(III) and La(III) analogues.^{41c} The reaction time and product selectivity showed that the aldehyde reactivity follows the order: linear > aromatic > citral.^{41c} Similar catalytic studies were performed with Ln-MOFs containing the same linker but having different structural topologies.^{41a} They showed that the catalytic activity depends strongly on the network structure, with only a minor influence for the lanthanide ion.^{41a}

Other Reactions. The acetalization of benzaldehyde with methanol in the presence of [Ln₂(dpa)₃] gave mainly 1,1-dimethoxytoluene.⁴⁹ The most active catalyst was [Tb₂(dpa)₃], giving a 78% conversion in 10 h.⁴⁹ The conversion was only 22% when the reaction was run using excess water.⁴⁹ This indicates the poisoning of the active sites as a result of the coordination of water molecules to the Tb(III) ions.

The Aldol reaction of cyclohexanone with various aldehydes was performed in the presence of [Tb₆(H₃L)₄(NO₃)₉·3H⁺]⁶⁺.^{40d} Here, the highest conversion of 80% was achieved with 4-nitrobenzaldehyde, with a 2:1 syn:anti ratio. Size selectivity and fluorescent titration studies showed that the aldol reaction occurs within the framework's octahedral cavities.^{40d}

Other reactions catalyzed by Ln-MOFs include ring opening,^{41d} the conversion of xylose to furfural,⁵⁰ Diels–Alder and Strecker reactions,^{40b} polymerization of isoprene,⁵¹ and reduction of nitroaromatics.^{41b} Notably, the compound [Y(H₂cmp)(H₂O)] (H₃cmp = N-(carboxymethyl)iminodimethylphosphonic acid) has many accessible terminal P–OH groups on the surface of the crystals.⁵⁰ This material gave the highest conversion (83%) and the highest selectivity (84%) in the cyclodehydration of xylose to furfural.⁵⁰

Although lanthanide-based luminescence is a common property of Ln-MOFs, its application in photochemical reactions is hardly explored. Only one study reports that Eu-MOFs may work as efficient catalysts under UV light irradiation.⁵² Time-resolved emission and adsorption spectroscopy together with confocal microscopy indicated a photo-induced electron transfer between excited Eu-MOFs nanoparticles and various organic molecules.⁵²

Recently, a series of Ln-MOFs based on 2-acetamidoterephthalic acid with channels of ca. 10 Å × 10 Å were reported as active catalysts for the nitroaldol reaction of different aldehydes.^{40a} The highest activity, up to 50% yield, was obtained for the Sm-MOF. It was concluded that the catalytic activity occurs mainly at the MOF surface and that the higher electronegativity of Sm(III) compared with those of La(III) and Ce(III) accounts for the higher activity of Sm-MOF.^{40a}

■ SUMMARY

This review summarized the main synthetic strategies applied for designing and making porous and highly stable Ln-based MOFs. The examples discussed demonstrate that progress is being made in the rational design of porous structures built

from lanthanide ions. The isorecticular and building-block approaches are the most efficient ones because they give the possibility to finely tune the pore sizes and geometries of the MOF. However, the MOFs obtained by these methods have not been used yet for catalytic applications.

A few Ln-based MOFs were used as catalysts for various organic reactions. The synthetic strategies for making Ln-MOFs catalysts are far less developed. They are usually focused on combining the Lewis acidity of the lanthanide ions with acidic or basic functionalities on the organic linker, to promote faster and more efficient substrate activation. The Ln-MOFs with high concentration acid sites are promising to be effective, recyclable, and reusable solids catalysts, especially in oxidation and cyanosilylation reactions. However, in most cases, the substrate activation occurs at MOF surface rather than in the pores. By sharp contrast, MOFs with both acid and basic sites are much more reactive and pore size dependent catalytic activity was demonstrated in a few cases. Therefore, we foresee that the heterogenisation of lanthanide Lewis acids in the confined space of MOFs by applying the isorecticular or building-block approaches using organic linkers with basic functionalities will open new opportunities for designing and developing novel catalytic Ln-MOFs materials.

AUTHOR INFORMATION

Corresponding Author

*E-mail: s.grecea@uva.nl.

Present Address

[§](C.P.) IRCELYON, Institut de Recherches sur la Catalyse et l'Environnement de Lyon, 69626 Villeurbanne, France.

Notes

The authors declare no competing financial interest.

ACKNOWLEDGMENTS

This work is part of the Research Priority Area Sustainable Chemistry of the University of Amsterdam, <http://suschem.uva.nl>.

REFERENCES

- (1) Yamamoto, H.; Shibasaki, M.; Yamada, K. I.; Yoshikawa, N. *Lewis acids in organic synthesis*; Wiley VCH: Weinheim, 2008.
- (2) Kobayashi, S.; Uchiro, H.; Fujishita, Y.; Shiina, I.; Mukaiyama, T. *J. Am. Chem. Soc.* **1991**, *113* (11), 4247–4252.
- (3) Walker, M.; Balshi, M.; Lauster, A.; Birmingham, P. An Environmentally Benign Process for Friedel–Crafts Acylation. *Proceedings of the 4th Annual Green Chemistry and Engineering Conference*; Washington, DC, June 27–29, 2000; pp 41–46.
- (4) Engberts, J.; Feringa, B. L.; Keller, E.; Otto, S. *Recl. Trav. Chim. Pays-Bas* **1996**, *115* (11–12), 457–464.
- (5) Kobayashi, S.; Manabe, K. *Pure Appl. Chem.* **2000**, *72* (7), 1373–1380.
- (6) (a) Arnold, P. L.; McMullon, M. W.; Rieb, J.; Kuehn, F. E. *Angew. Chem., Int. Ed.* **2015**, *54* (1), 82–100. (b) Dantas Ramos, A. L.; Tanase, S.; Rothenberg, G. *Quim. Nova* **2014**, *37* (1), 123–133. (c) Liu, W.; Tang, X. *Struct. Bonding* **2014**, *163*, 29–74. (d) Zhang, T.; Lin, W. *Chem. Soc. Rev.* **2014**, *43* (16), 5982–5993.
- (7) (a) Yao, Y.; Nie, K. *Encyclopedia of inorganic and bioinorganic chemistry*; Wiley VCH: Weinheim, 2012; DOI: [10.1002/9781119951438.eibc2046](https://doi.org/10.1002/9781119951438.eibc2046), (b) Edelmann, F. T. *Struct. Bonding (Berlin, Ger.)* **2010**, *137*, 109–163. (c) Edelmann, F. T. In *Organolanthoid Chemistry: Synthesis, Structure, Catalysis*; Herrmann, W. A., Ed.; Springer: Berlin, 2005; Vol. 179, pp 247–276. (d) Edelmann, F. T. *Chem. Soc. Rev.* **2012**, *41* (23), 7657–7672.
- (8) (a) Baba, Y.; Kubota, F.; Kamiya, N.; Goto, M. *J. Chem. Eng. Jpn.* **2011**, *44* (10), 679–685. (b) Chen, J. I. *Application of Ionic Liquids on Rare Earth Green Separation and Utilization*. Springer: Berlin, 2016.
- (9) (a) Corma, A.; Garcia, H. *Chem. Rev.* **2003**, *103* (11), 4307–4365. (b) Kobayashi, S.; Manabe, K. *Acc. Chem. Res.* **2002**, *35* (4), 209–217.
- (10) (a) Farrusseng, D. *Metal–Organic Frameworks*; Wiley-VCH: Weinheim, 2011. (b) Farrusseng, D.; Aguado, S.; Pinel, C. *Angew. Chem., Int. Ed.* **2009**, *48* (41), 7502–7513. (c) Lin, X.; Champness, N. R.; Schroder, M. *Top. Curr. Chem.* **2009**, *293*, 35–76.
- (11) (a) Fang, W.-H.; Zhang, L.; Zhang, J.; Yang, G.-Y. *Chem. - Eur. J.* **2016**, *22* (8), 2611–2615. (b) Qin, J.-H.; Ma, B.; Liu, X.-F.; Lu, H.-L.; Dong, X.-Y.; Zang, S.-Q.; Hou, H. *Dalton Trans.* **2015**, *44* (33), 14594–14603. (c) Xu, H.; Cao, C.-S.; Zhao, B. *Chem. Commun.* **2015**, *51* (51), 10280–10283. (d) Gustafsson, M.; Bartoszewicz, A.; Martin-Matute, B.; Sun, J. L.; Grins, J.; Zhao, T.; Li, Z. Y.; Zhu, G. S.; Zou, X. D. *Chem. Mater.* **2010**, *22* (11), 3316–3322. (e) Plessius, R.; Kromhout, R.; Ramos, A. L. D.; Ferbinteanu, M.; Mittelmeijer-Hazeleger, M. C.; Krishna, R.; Rothenberg, G.; Tanase, S. *Chem. - Eur. J.* **2014**, *20* (26), 7922–7925.
- (12) (a) Corkery, R. W. *Curr. Opin. Colloid Interface Sci.* **2008**, *13* (4), 288–302. (b) Cui, Y.; Chen, B.; Qian, G. *Coord. Chem. Rev.* **2014**, *273*, 76–86. (c) Cui, Y.; Chen, B.; Qian, G. *Struct. Bonding* **2013**, *157*, 27–88. (d) Fordham, S.; Wang, X.; Bosch, M.; Zhou, H.-C. *Struct. Bonding* **2014**, *163*, 1–27. (e) Li, B.; Chen, B. Porous Lanthanide Metal–Organic Frameworks for Gas Storage and Separation. *Struct. Bonding* **2014**, *163*, 75–107. (f) Ma, L.; Lin, W. *Top. Curr. Chem.* **2009**, *293*, 175–205. (g) Tong, X.-L.; Lin, H.-L.; Xin, J.-H.; Liu, F.; Li, M.; Zhu, X.-P. *J. Nanomater.* **2013**, *2013*, Article No. 616501. (h) Zhang, X.; Wang, W.; Hu, Z.; Wang, G.; Uvdal, K. *Coord. Chem. Rev.* **2015**, *284*, 206–235. (i) Zhang, Z.; Zheng, Z. *Struct. Bonding* **2014**, *163*, 297–367.
- (13) (a) Allendorf, M. D.; Bauer, C. A.; Bhakta, R. K.; Houk, R. J. T. *Chem. Soc. Rev.* **2009**, *38* (5), 1330–1352. (b) Rocha, J.; Carlos, L. D.; Paz, F. A. A.; Ananias, D. *Chem. Soc. Rev.* **2011**, *40* (2), 926–940. (c) Chen, Y.; Ma, S. Q. *Rev. Inorg. Chem.* **2012**, *32* (2–4), 81–100.
- (14) Yao, Q.; Gomez, A. B.; Su, J.; Pascanu, V.; Yun, Y.; Zheng, H.; Chen, H.; Liu, L.; Abdelhamid, H. N.; Martin-Matute, B.; Zou, X. *Chem. Mater.* **2015**, *27* (15), 5332–5339.
- (15) Reineke, T. M.; Eddaoudi, M.; O'Keeffe, M.; Yaghi, O. M. *Angew. Chem., Int. Ed.* **1999**, *38* (17), 2590–2594.
- (16) Reineke, T. M.; Eddaoudi, M.; Fehr, M.; Kelley, D.; Yaghi, O. M. *J. Am. Chem. Soc.* **1999**, *121* (8), 1651–1657.
- (17) He, H. Y.; Yuan, D. Q.; Ma, H. Q.; Sun, D. F.; Zhang, G. Q.; Zhou, H. C. *Inorg. Chem.* **2010**, *49* (17), 7605–7607.
- (18) Wang, Y. L.; Jiang, Y. L.; Liu, Q. Y.; Tan, Y. X.; Wei, J. J.; Zhang, J. *CrystEngComm* **2011**, *13* (15), 4981–4987.
- (19) (a) Han, Y.; Li, X.; Li, L.; Ma, C.; Shen, Z.; Song, Y.; You, X. *Inorg. Chem.* **2010**, *49* (23), 10781–10787. (b) He, H.; Ma, H.; Sun, D.; Zhang, L.; Wang, R.; Sun, D. *Cryst. Growth Des.* **2013**, *13* (7), 3154–3161. (c) Sibille, R.; Mazet, T.; Malaman, B.; Francois, M. *Chem. - Eur. J.* **2012**, *18* (41), 12970–12973. (d) Zhang, W.-Z. *Acta Crystallogr., Sect. E: Struct. Rep. Online* **2006**, *62*, m1600–m1602.
- (20) (a) Cai, B.; Yang, P.; Dai, J.-W.; Wu, J.-Z. *CrystEngComm* **2011**, *13* (3), 985–991. (b) Gu, J.-Z.; Gao, Z.-Q. *J. Chem. Crystallogr.* **2012**, *42* (3), 283–289. (c) Yang, P.; Wu, J.-Z.; Yu, Y. *Inorg. Chim. Acta* **2009**, *362* (6), 1907–1912. (d) Zheng, X. J.; Jin, L. P. *J. Chem. Crystallogr.* **2005**, *35* (11), 865–869.
- (21) (a) Guo, X. D.; Zhu, G. S.; Fang, Q. R.; Xue, M.; Tian, G.; Sun, J. Y.; Li, X. T.; Qiu, S. L. *Inorg. Chem.* **2005**, *44* (11), 3850–3855. (b) Han, Y.-F.; Zhou, X.-H.; Zheng, Y.-X.; Shen, Z.; Song, Y.; You, X.-Z. *CrystEngComm* **2008**, *10* (9), 1237–1242. (c) Lin, Z.; Singh-Wilmoth, M. A.; Cahill, C. L.; Andrews, M.; Taylor, R. *Eur. J. Inorg. Chem.* **2012**, *2012* (28), 4419–4426. (d) Sienkiewicz-Gromiuk, J.; Rzaczyńska, Z. *J. Therm. Anal. Calorim.* **2013**, *112* (2), 877–884. (e) Wang, Y. B.; Zhuang, W. J.; Jin, L. P.; Lu, S. Z. *J. Mol. Struct.* **2004**, *705* (1–3), 21–27. (f) Jia, L.-N.; Hou, L.; Wei, L.; Jing, X.-J.; Liu, B.; Wang, Y.-Y.; Shi, Q.-Z. *Cryst. Growth Des.* **2013**, *13* (4), 1570–1576.

- (22) Reineke, T. M.; Eddaoudi, M.; Moler, D.; O'Keeffe, M.; Yaghi, O. M. *J. Am. Chem. Soc.* **2000**, *122* (19), 4843–4844.
- (23) Jiang, H. L.; Tsumori, N.; Xu, Q. *Inorg. Chem.* **2010**, *49* (21), 10001–10006.
- (24) (a) Rosi, N. L.; Kim, J.; Eddaoudi, M.; Chen, B. L.; O'Keeffe, M.; Yaghi, O. M. *J. Am. Chem. Soc.* **2005**, *127* (5), 1504–1518. (b) Guo, X. D.; Zhu, G. S.; Li, Z. Y.; Sun, F. X.; Yang, Z. H.; Qiu, S. L. *Chem. Commun.* **2006**, No. 30, 3172–3174. (c) Guo, X. D.; Zhu, G. S.; Li, Z. Y.; Chen, Y.; Li, X. T.; Qiu, S. L. *Inorg. Chem.* **2006**, *45* (10), 4065–4070. (d) Khan, N. A.; Haque, M. M.; Jhung, S. H. *Eur. J. Inorg. Chem.* **2010**, *2010* (31), 4975–4981.
- (25) Luo, J. H.; Xu, H. W.; Liu, Y.; Zhao, Y. S.; Daemen, L. L.; Brown, C.; Timofeeva, T. V.; Ma, S. Q.; Zhou, H. C. *J. Am. Chem. Soc.* **2008**, *130* (30), 9626.
- (26) Mu, B.; Li, F.; Huang, Y. G.; Walton, K. S. *J. Mater. Chem.* **2012**, *22* (20), 10172–10178.
- (27) Devic, T.; Serre, C.; Audebrand, N.; Marrot, J.; Ferey, G. *J. Am. Chem. Soc.* **2005**, *127* (37), 12788–12789.
- (28) (a) Lin, Z. J.; Zou, R. Q.; Xia, W.; Chen, L. J.; Wang, X. D.; Liao, F. H.; Wang, Y. X.; Lin, J. H.; Burrell, A. K. *J. Mater. Chem.* **2012**, *22* (39), 21076–21084. (b) Duan, J.; Higuchi, M.; Horike, S.; Foo, M. L.; Rao, K. P.; Inubushi, Y.; Fukushima, T.; Kitagawa, S. *Adv. Funct. Mater.* **2013**, *23* (28), 3525–3530. (c) Duan, J.; Higuchi, M.; Krishna, R.; Kiyonaga, T.; Tsutsumi, Y.; Sato, Y.; Kubota, Y.; Takata, M.; Kitagawa, S. *Chem. Sci.* **2014**, *5* (2), 660–666. (d) He, Y.; Xiang, S.; Zhang, Z.; Xiong, S.; Fronczek, F. R.; Krishna, R.; O'Keeffe, M.; Chen, B. *Chem. Commun.* **2012**, *48* (88), 10856–10858. (e) Lin, Z.; Zou, R.; Liang, J.; Xia, W.; Xia, D.; Wang, Y.; Lin, J.; Hu, T.; Chen, Q.; Wang, X.; Zhao, Y.; Burrell, A. K. *J. Mater. Chem.* **2012**, *22* (16), 7813–7818.
- (29) (a) Ma, S. Q.; Yuan, D. Q.; Wang, X. S.; Zhou, H. C. *Inorg. Chem.* **2009**, *48* (5), 2072–2077. (b) Zhang, Z. H.; Wan, S. Y.; Okamura, T.; Sun, W. Y.; Ueyama, N. Z. *Anorg. Allg. Chem.* **2006**, *632* (4), 679–683.
- (30) Park, Y. K.; Choi, S. B.; Kim, H.; Kim, K.; Won, B. H.; Choi, K.; Choi, J. S.; Ahn, W. S.; Won, N.; Kim, S.; Jung, D. H.; Choi, S. H.; Kim, G. H.; Cha, S. S.; Jhon, Y. H.; Yang, J. K.; Kim, J. *Angew. Chem., Int. Ed.* **2007**, *46* (43), 8230–8233.
- (31) (a) Datcu, A.; Roques, N.; Jubera, V.; Imaz, I.; MasPOCH, D.; Sutter, J. P.; Rovira, C.; Veciana, J. *Chem. - Eur. J.* **2011**, *17* (13), 3644–3656. (b) Datcu, A.; Roques, N.; Jubera, V.; MasPOCH, D.; Fontrodona, X.; Wurst, K.; Imaz, I.; Mouchaham, G.; Sutter, J. P.; Rovira, C.; Veciana, J. *Chem. - Eur. J.* **2012**, *18* (1), 152–162. (c) Roques, N.; MasPOCH, D.; Imaz, I.; Datcu, A.; Sutter, J. P.; Rovira, C.; Veciana, J. *Chem. Commun.* **2008**, No. 27, 3160–3162.
- (32) (a) Su, S. Q.; Chen, W.; Qin, C.; Song, S. Y.; Guo, Z. Y.; Li, G. H.; Song, X. Z.; Zhu, M.; Wang, S.; Hao, Z. M.; Zhang, H. J. *Cryst. Growth Des.* **2012**, *12* (4), 1808–1815. (b) Zheng, B.; Zhang, D. J.; Peng, Y.; Huo, Q. S.; Liu, Y. L. *Inorg. Chem. Commun.* **2012**, *16*, 70–73.
- (33) Guo, X. D.; Zhu, G. S.; Sun, F. X.; Li, Z. Y.; Zhao, X. J.; Li, X. T.; Wang, H. C.; Qiu, S. L. *Inorg. Chem.* **2006**, *45* (6), 2581–2587.
- (34) (a) Alezi, D.; Peedikakkal, A. M. P.; Weselinski, L. J.; Guillerm, V.; Belmabkhout, Y.; Cairns, A. J.; Chen, Z.; Wojtas, L.; Eddaoudi, M. *J. Am. Chem. Soc.* **2015**, *137* (16), 5421–5430. (b) Luebke, R.; Belmabkhout, Y.; Weselinski, L. J.; Cairns, A. J.; Alkordi, M.; Norton, G.; Wojtas, L.; Adil, K.; Eddaoudi, M. *Chem. Sci.* **2015**, *6* (7), 4095–4102. (c) Xue, D.-X.; Belmabkhout, Y.; Shekha, O.; Jiang, H.; Adil, K.; Cairns, A. J.; Eddaoudi, M. *J. Am. Chem. Soc.* **2015**, *137* (15), 5034–5040. (d) Guillerm, V.; Weselinski, L. J.; Belmabkhout, Y.; Cairns, A. J.; D'Elia, V.; Wojtas, L.; Adil, K.; Eddaoudi, M. *Nat. Chem.* **2014**, *6* (8), 673–680.
- (35) Xue, D.-X.; Cairns, A. J.; Belmabkhout, Y.; Wojtas, L.; Liu, Y.; Alkordi, M. H.; Eddaoudi, M. *J. Am. Chem. Soc.* **2013**, *135* (20), 7660–7667.
- (36) Hoskins, B. F.; Robson, R. *J. Am. Chem. Soc.* **1990**, *112* (4), 1546–1554.
- (37) Chandler, B. D.; Cramb, D. T.; Shimizu, G. K. H. *J. Am. Chem. Soc.* **2006**, *128* (32), 10403–10412.
- (38) (a) Tanase, S.; Mittelmeijer-Hazeleger, M. C.; Rothenberg, G.; Mathoniere, C.; Jubera, V.; Smits, J. M. M.; de Gelder, R. *J. Mater. Chem.* **2011**, *21* (39), 15544–15551. (b) Tanase, S.; Prins, F.; Smits, J. M. M.; de Gelder, R. *CrystEngComm* **2006**, *8* (12), 863–865.
- (39) Gao, Y.; Broersen, R.; Hageman, W.; Yan, N.; Mittelmeijer-Hazeleger, M. C.; Rothenberg, G.; Tanase, S. *J. Mater. Chem. A* **2015**, *3* (44), 22347–22352.
- (40) (a) Karmakar, A.; Hazra, S.; Guedes da Silva, M. F. C.; Paul, A.; Pombeiro, A. J. L. *CrystEngComm* **2016**, *18* (8), 1337–1349. (b) Liu, Y.; Mo, K.; Cui, Y. *Inorg. Chem.* **2013**, *52* (18), 10286–10291. (c) Wu, P.; Wang, J.; Li, Y.; He, C.; Xie, Z.; Duan, C. *Adv. Funct. Mater.* **2011**, *21* (14), 2788–2794. (d) Wu, X.; Lin, Z. H.; He, C.; Duan, C. Y. *New J. Chem.* **2012**, *36* (1), 161–167.
- (41) (a) D'Vries, R. F.; de la Pena-O'Shea, V. A.; Snejko, N.; Iglesias, M.; Gutierrez-Puebla, E.; Monge, M. A. *Cryst. Growth Des.* **2012**, *12*, 5535–5545. (b) D'Vries, R. F.; Iglesias, M.; Snejko, N.; Alvarez-Garcia, S.; Gutierrez-Puebla, E.; Monge, M. A. *J. Mater. Chem.* **2012**, *22* (3), 1191–1198. (c) D'Vries, R. F.; Iglesias, M.; Snejko, N.; Gutierrez-Puebla, E.; Monge, M. A. *Inorg. Chem.* **2012**, *51*, 11349–11355. (d) Evans, O. R.; Ngo, H. L.; Lin, W. B. *J. Am. Chem. Soc.* **2001**, *123* (42), 10395–10396. (e) Gandara, F.; de Andres, A.; Gomez-Lor, B.; Gutierrez-Puebla, E.; Iglesias, M.; Monge, M. A.; Proserpio, D. M.; Snejko, N. *Cryst. Growth Des.* **2008**, *8* (2), 378–380. (f) Gandara, F.; Garcia-Cortes, A.; Cascales, C.; Gomez-Lor, B.; Gutierrez-Puebla, E.; Iglesias, M.; Monge, A.; Snejko, N. *Inorg. Chem.* **2007**, *46* (9), 3475–3484. (g) Gandara, F.; Gutierrez-Puebla, E.; Iglesias, M.; Snejko, N.; Monge, M. A. *Cryst. Growth Des.* **2010**, *10* (1), 128–134. (h) Gandara, F.; Puebla, E. G.; Iglesias, M.; Proserpio, D. M.; Snejko, N.; Monge, M. A. *Chem. Mater.* **2009**, *21* (4), 655–661.
- (42) Xia, Q. H.; Ge, H. Q.; Ye, C. P.; Liu, Z. M.; Su, K. X. *Chem. Rev.* **2005**, *105* (5), 1603–1662.
- (43) Sen, R.; Saha, D.; Koner, S. *Catal. Lett.* **2012**, *142* (1), 124–130.
- (44) Snejko, N.; Cascales, C.; Gomez-Lor, B.; Gutierrez-Puebla, E.; Iglesias, M.; Ruiz-Valero, C.; Monge, M. A. *Chem. Commun.* **2002**, No. 13, 1366–1367.
- (45) (a) Bernini, M. C.; Gandara, F.; Iglesias, M.; Snejko, N.; Gutierrez-Puebla, E.; Brusau, E. V.; Narda, G. E.; Monge, M. A. *Chem. - Eur. J.* **2009**, *15* (19), 4896–4905. (b) Han, J. W.; Hill, C. L. *J. Am. Chem. Soc.* **2007**, *129* (49), 15094–15095.
- (46) (a) Hanquet, G.; Salom-Roig, X. J.; Gressot-Kempf, L.; Lanners, S.; Solladie, G. *Tetrahedron: Asymmetry* **2003**, *14* (10), 1291–1301. (b) Solladie, G. *Heteroat. Chem.* **2002**, *13* (5), 443–452.
- (47) Gregory, R. J. H. *Chem. Rev.* **1999**, *99* (12), 3649–3682.
- (48) Tsuruta, H.; Yamaguchi, K.; Imamoto, T. *Chem. Commun.* **1999**, No. 17, 1703–1704.
- (49) Ren, Y. W.; Liang, J. X.; Lu, J. X.; Cai, B. W.; Shi, D. B.; Qi, C. R.; Jiang, H. F.; Chen, J.; Zheng, D. *Eur. J. Inorg. Chem.* **2011**, *2011* (28), 4369–4376.
- (50) Cunha-Silva, L.; Lima, S.; Ananias, D.; Silva, P.; Mafra, L.; Carlos, L. D.; Pillinger, M.; Valente, A. A.; Paz, F. A. A.; Rocha, J. J. *J. Mater. Chem.* **2009**, *19* (17), 2618–2632.
- (51) Vitorino, M. J.; Devic, T.; Tromp, M.; Ferey, G.; Visseaux, M. *Macromol. Chem. Phys.* **2009**, *210* (22), 1923–1932.
- (52) Choi, J. R.; Tachikawa, T.; Fujitsuka, M.; Majima, T. *Langmuir* **2010**, *26* (13), 10437–10443.